energies

MDPI

Article

Optimal Control Strategy for Series Hybrid Electric Vehicles in the Warm-Up Process

Da Wang *, Chuanxue Song, Yulong Shao, Shixin Song *, Silun Peng and Feng Xiao

College of Automotive Engineering, Jilin University, Changchun 130000, China; songchx@126.com (C.S.); shaoyl13@mails.jlu.edu.cn (Y.S.); pengsilun@jlu.edu.cn (S.P.); xiaofengjl@jlu.edu.cn (F.X.)

* Correspondence: wangda_gspeed@jlu.edu.cn (D.W.); songshx0202@126.com (S.S.)

Received: 8 April 2018; Accepted: 27 April 2018; Published: 28 April 2018

Abstract: To address the problems of low efficiency and high fuel consumption during the cold start and warm-up processes of internal combustion engines, a series hybrid electric vehicle was selected as the research object and two optimal control strategies were designed. A bench test was performed to determine the following: (a) the influence of engine coolant temperature on effective thermal efficiency; and (b) the relationship between engine operating conditions and coolant temperature increase rate. On the basis of the test results, two sets of warm-up process optimization control strategies were designed using a dynamic programming method and a fuzzy control method based on equivalent consumption minimization strategy (ECMS). The test results show that the fuzzy control method for the coolant temperature can effectively shorten the time required to warm up the engine, and the energy consumption of warm-up process can be reduced by nearly 10% through the dynamic programming method.

Keywords: series hybrid electric vehicle; warm-up process optimization; fuzzy control; dynamic programming; energy management strategy

1. Introduction

The ideal working temperature of the internal combustion engine is generally 373 K~398 K (80~105 degrees Celsius) [1]. When engine temperature is lower than the ideal operating temperature, the engine exhibits high mechanical resistance, considerable heat transfer loss and poor fuel vaporization, thereby eventually increasing engine fuel consumption and pollutant emissions [2–5]. Modern vehicle internal combustion engines are equipped with control devices, such as thermostats, which can help shorten the engine's warming time. However, changing the engine coolant temperature from ambient temperature to the ideal working temperature still takes several minutes. If in a high-latitude cold environment, the warming time could be longer than 15–30 min, and then the energy consumed during the process cannot be disregarded.

Existing research shows that the warm-up process of hybrid vehicles also experiences the problems of high fuel consumption and high pollutant emissions [6–8]. The energy management control strategy of hybrid electric vehicles (HEVs) is designed according to the efficiency characteristics of the internal combustion engine at an ideal temperature. Thus, energy economy in a low-temperature environment is not ideal [9,10]. Researchers have focused on this issue and achieved several significant results. Reference [11] studied the influences of the driving mode of engines and regenerative braking on heating time. References [12,13] found that application model predictive control shortens the after-treatment device warm-up time of an HEV. References [14,15] considered the heating requirements of cabins and improved the load control strategy of hybrid vehicles. Reference [16,17] considered the low-temperature characteristics of power batteries in energy management strategies. References [18,19] presented the design and research of a simulation model for the warm-up process

of a hybrid vehicle. Reference [20] designs a control strategy including dynamic programming and model predictive control, which shows that the RCCI (Reactivity Controlled Compression Ignition) engine offers more fuel economy improvement in more aggressive driving cycles, and sub-optimal fuel economy is achieved by predicting the vehicle speed profile for a time horizon of 70 s.

At different output power and coolant temperatures, the engine's temperature increase rate and efficiency are also different. Considerable power can shorten warm-up time but increase power loss per unit time. In conventional vehicles, the driver directly controls the engine load. The speed and load of the engine depend on road conditions and driving intent, and thus, achieving optimal control of the warm-up process is difficult. For a series HEV, the engine is only connected to the generator and both form an auxiliary power unit (APU). No mechanical coupling occurs between the engine and the wheels, which makes optimizing the control of the warm-up process possible [21–23]. The current study selects a series HEV as the research object and obtains the efficiency characteristics of engines at different temperatures and temperature increase characteristics under varying working conditions by using the test method. Then, to reduce energy consumption during the warm-up process and shorten warm-up time, a dynamic programming method and a fuzzy control method are used to establish an optimal control strategy for the two types of HEV warm-up process. Finally, the optimization control strategy is verified through experiments.

2. Design of the Powertrain Testing Bench

This article selects a small series HEV passenger vehicle (parameters as shown Table 1) as the research object and establishes a powertrain test platform, as shown in Figure 1. The car is equipped with a 1.0 L three-cylinder gasoline engine, a 30 kW generator and a 40 kW drive motor.

Table 1. Technical parameters of the Series hybrid electric vehicle (HEV).

Parameter	Value	Units
Curb weight	1400	Kg
Layout	Front-engine front-drive	/
Length × width × height	4600 × 1785 × 1435	mm
Wheelbase	2675	mm
Tire	205/55R16	/
Drag coefficient	0.32	/
Frontal area	1.98	m^2
Battery capacity	15.8	kWh

The test bench consists of the engine, generator, drive motor, electric eddy current dynamometer, gearbox, flywheel, power analyzer, battery simulation system, fuel consumption instrument, coolant heat exchange system, rapid prototype controller, computer, etc.

The drive subsystem consists of a drive motor, a gearbox, a flywheel and an eddy current dynamometer that simulates road resistance and drive power.

The generation subsystem consists of an engine, a generator, a fuel tank and a fuel consumption instrument. This subsystem can provide electrical energy and measure fuel consumption.

The high-voltage power subsystem consists of a battery simulation system, a power analyser, a motor controller and a generator controller. The subsystem can provide a suitable DC voltage, measure power consumption, calculate the efficiency of the motor and controller as well as simulate the SOC of a real battery.

The cooling subsystem consists of a coolant heat-exchanging system, an electric pump and a radiator. The coolant heat-exchanging system controls the engine coolant at a set level, whilst the electric pump and radiator cool the drive motor and generator.

The control subsystem consists of a computer and a rapid prototype controller that controls the output of the engine, generator and drive motor as well as collects data from the sensors.

The performance parameters of each component are listed in Table 2.

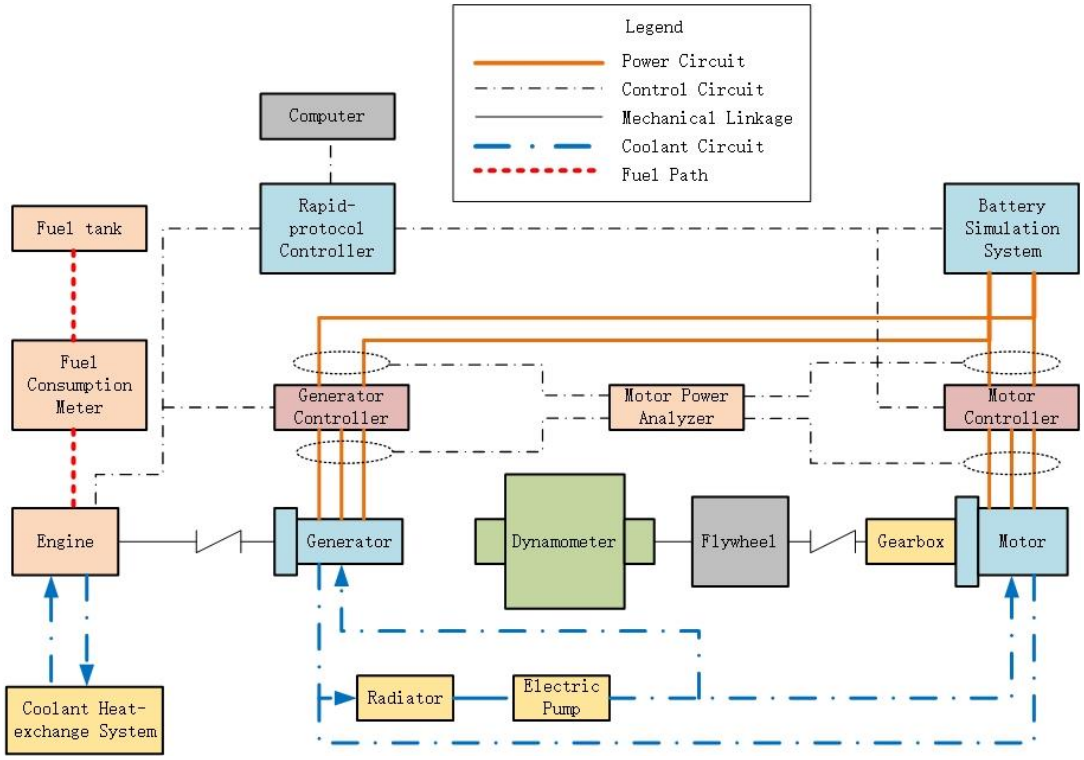

(**a**) Schematic

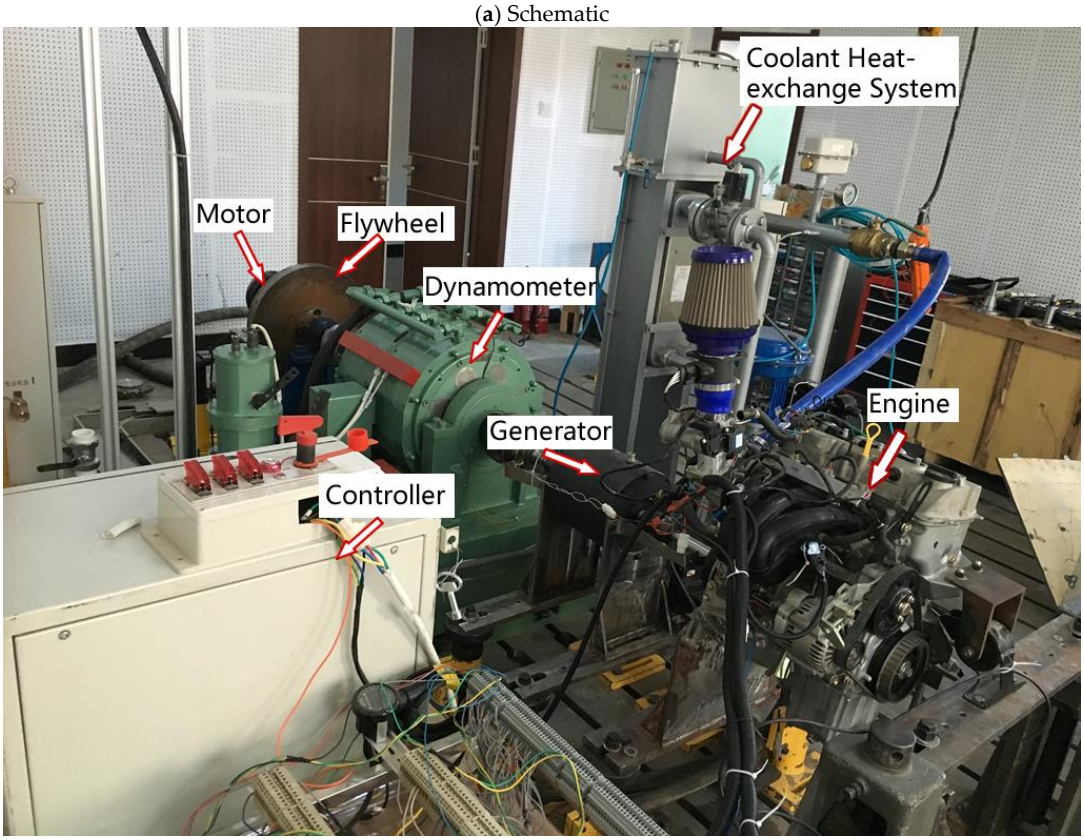

(**b**) Physical Photo

Figure 1. Serial HEV powertrain testing platform.

Table 2. Serial HEV powertrain testing platform parameters.

Items	Parameter
Dynamometer	
Type	CAMA CW-260
Rated power/kW	260
Maximum speed/r/min	7500
Brake torque/Nm	1395
Fuel Consumption Meter	
Type	FCM-1
Flow rate/kg/h	0~100
Measurement accuracy/%FS	0.12
Measurement repeatability/%FS	0.05
Coolant Heat-Exchange System	
Type	SHW-300
Capacity engine power/kW	300
Temperature rate/°C	20~130
Control accuracy/°C	$<\pm 2$
Measurement accuracy/°C	$<\pm 0.5$
Battery Simulation System	
Type	AVL e-Storage
Power/kW	−160~160
Output voltage/V	0~650
Maximum current/A	600
Measurement accuracy/%FS	$<\pm 0.02$
Rapid-Prototype Controller	
Type	Motohawk ECM565-128
Processor	Freescale MPC565
Flash/kB	1024
RAM/kB	548
EEPROM/kB	512
Motor Power Analyzer	
Type	YOKOGAWA WT-1800
Basic power accuracy/%	± 0.1
DC Accuracy/%	± 0.05
Band-wide/MHz	5
Sample rate/MS/s	2
Engine	
Model	K10B
Cylinder type	Inline 3-cylinder
Intake type	Natural aspiration
Displacement/mL	998
Compression ratio	10.2
Power/kW	52
Torque/Nm	90
Generator	
Type	Permanent magnet synchronous
Rated power/kW	30
Rated torque/Nm	100
Maximum speed/r/min	6000
Voltage/V	200–400
Driving Motor	
Type	Permanent magnet synchronous
Power/kW	40
Torque/Nm	150
Maximum speed/r/min	10,000
Voltage/V	250–400

3. Engine Temperature Characteristic Measurement

The optimized range of the working condition points of the auxiliary power unit (APU) in serial HEV is the curve formed by connecting the most efficient condition points according to the equivalent consumption minimization strategy (ECMS) [24–27]. Moreover, the selection of the most efficient condition points is based on the engine efficiency characteristic map under an ideal working temperature, as shown Figure 2. When an engine is operating below the ideal temperature range, the efficiency of the internal combustion engine and the most efficient condition points that correspond to a certain power output will vary with temperature. If the warm-up control is based only on the ideal operating temperature without considering the realistic values, then it will negatively affect engine efficiency during the warm-up process [17].

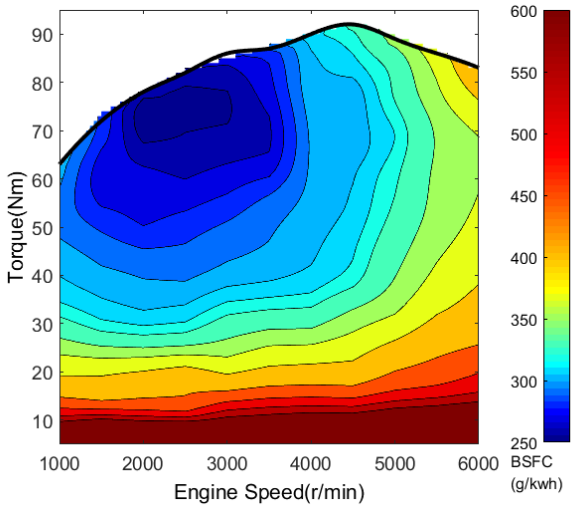

Figure 2. Engine efficiency map at the ideal coolant temperature (363 ± 5 K).

Figure 3a–d show the correlation among engine power output, engine speed and brake specific fuel consumption (BSFC). The effective fuel consumption rate is significantly reduced under all working conditions with an increase in the engine temperature from the ambient value to the ideal operating temperature. When temperature reaches 343 K, BSFC is basically stabilised around the value within the ideal operating temperature. Moreover, the corresponding ideal engine speed of a certain power output also increases with an increase in engine temperature.

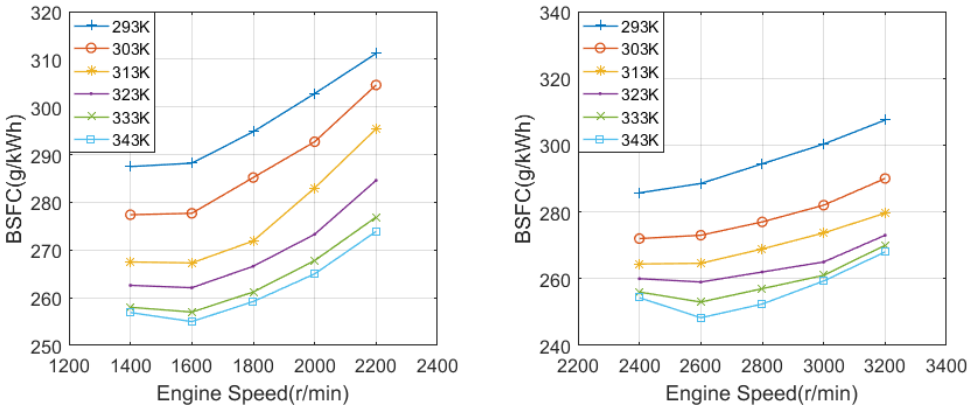

(**a**) 10 kW (**b**) 20 kW

Figure 3. *Cont.*

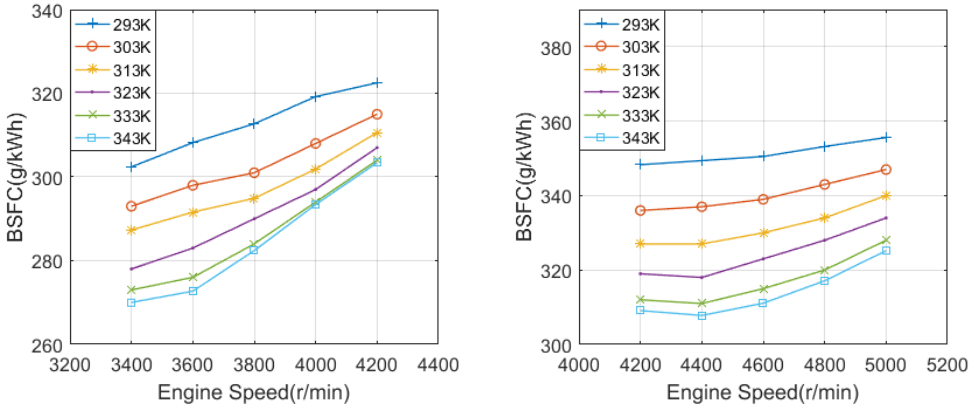

(**c**) 30 kW (**d**) 40 kW

Figure 3. Engine effective fuel consumption rate under different coolant temperatures.

The temperature increase of the internal combustion engine varies under different working conditions. The heat energy absorbed by the coolant is either from the heat transfer of combustion chambers, pistons and cylinder walls or generated by the friction of piston rings, rotating assembly, valve train and accessories, such as the coolant pump. Heat transfer is mainly influenced by engine volumetric efficiency and combustion heat release, whereas friction is influenced by engine speed and current engine temperature. Therefore, engine temperature increase is positively correlated with engine speed and engine load through qualitative analysis.

The engine temperature increase model is difficult to establish in physical form to make the simulation and verification processes highly efficient due to the complexity of the heat release and heat transfer mechanisms of internal combustion engines. In the current research, the correlations among engine power output, engine working conditions and temperature increase rate was measured quantitatively through engine bench tests, and a lookup table model of the engine temperature increase was established based on the bench test results. During the tests, ambient temperature was maintained within the range of 290 K~293 K, the engine was structured for real-life applications with the installed thermostat and radiator, and the coolant channels for internal cycles were also unblocked.

Figure 4a–d show the correlations among engine temperature, engine speed and coolant temperature increase under different engine power outputs within the range of 10 kW to 40 kW. The temperature increase of the coolant is mainly affected by the power output, and it increases along with an increase in engine speed. Engine temperature also influences the rate of temperature increase. Mechanical loss and internal friction decrease under the same power output and engine speed values with an increase in engine temperature. Therefore, the rate of temperature increase is relatively reduced.

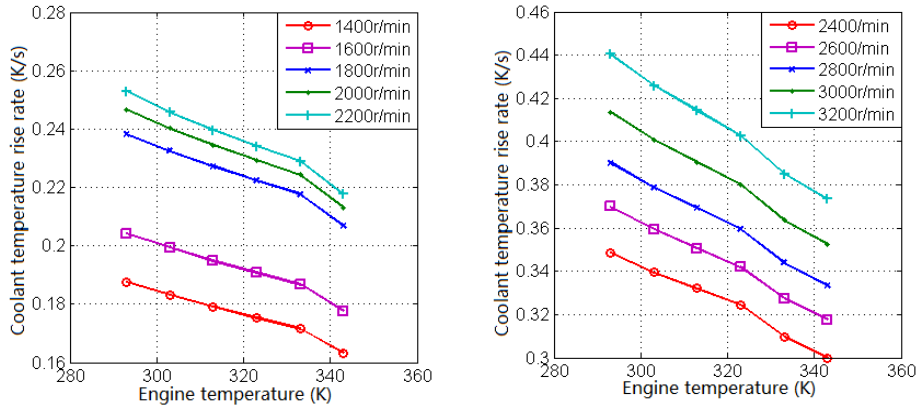

(**a**) 10 kW (**b**) 20 kW

Figure 4. *Cont.*

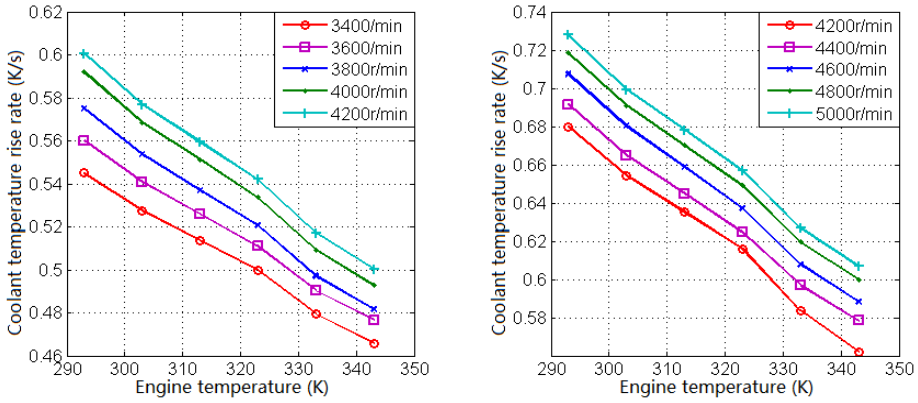

(**c**) 30 kW (**d**) 40 kW

Figure 4. The influence of coolant temperature and engine working conditions on the rate of coolant temperature-increase.

4. Dynamic Programming Strategy

From the perspective of engine temperature, control of the engine warm-up process can be regarded as an optimization topic with fixed starting and ending points, which are the ambient temperature value and the ideal operating temperature value or the thermostat opening temperature value, respectively. Meanwhile, the variation in the power output of the engine with time stands for different routes between two points. A certain sequence of power outputs that minimize overall fuel consumption during the engine warm-up process should be adopted because of the correlations among the four variables: power output, engine efficiency, temperature and time.

Dynamic programming is an effective means to achieve this type of optimal control sequence [28,29]. It discretizes continuous control on the timeline, converts it into a multi-stage decision-making process and finally decomposes it into a series of simple single-step decision-making problems. A global optimal solution is obtained by solving these simple problems and combining the overall optimization goals.

When solving the optimal control problem of the warm-up process using dynamic programming, the following assumptions and agreements should be made first:

(a) The starting and ending point of the warm-up process are the ambient temperature and the ideal operating temperature respectively, which are set to 293 K and 343 K in this research;
(b) During the warm-up process, the HEV is driven in serial hybrid mode, in which no connection occurs between engine speed and vehicle speed;
(c) Heat loss through the heater core is ignored, which means the coolant temperature will not decrease with time;
(d) The value of the engine power output is restricted as $P_{ICE} \in [10, 20]$, and the rounded-off value of the rate of temperature increase is within $\dot{T}_{ECT} \in [0.167, 0.333]$;
(e) The duration of the warm-up process will not exceed 300 s;
(f) The defined target for optimization is minimizing overall fuel consumption during the warm-up process, which is $Min\left\{\int_0^{300} \dot{m}_f dt\right\}$.

The dynamic programming model was established, and a total of 10 stages were divided in terms of time, with the duration of a single stage set as 30 s:

$$k = 1, 2 \ldots\ldots, 10 \quad (1)$$

State variable s_k is defined as the initial temperature of each stage:

$$\begin{cases} s_1 = 293 \\ s_2 = \{295, 298.5, 303\} \\ \ldots\ldots \\ s_6 = \{318, 320.5, \ldots\ldots, 340.5, 343\} \\ \ldots\ldots \\ s_{10} = \{338, 340.5, 343\} \\ s_{11} = 343 \end{cases} \tag{2}$$

Figure 5 shows the definitions of stage division and state variable of the dynamic programming model of the warm-up process.

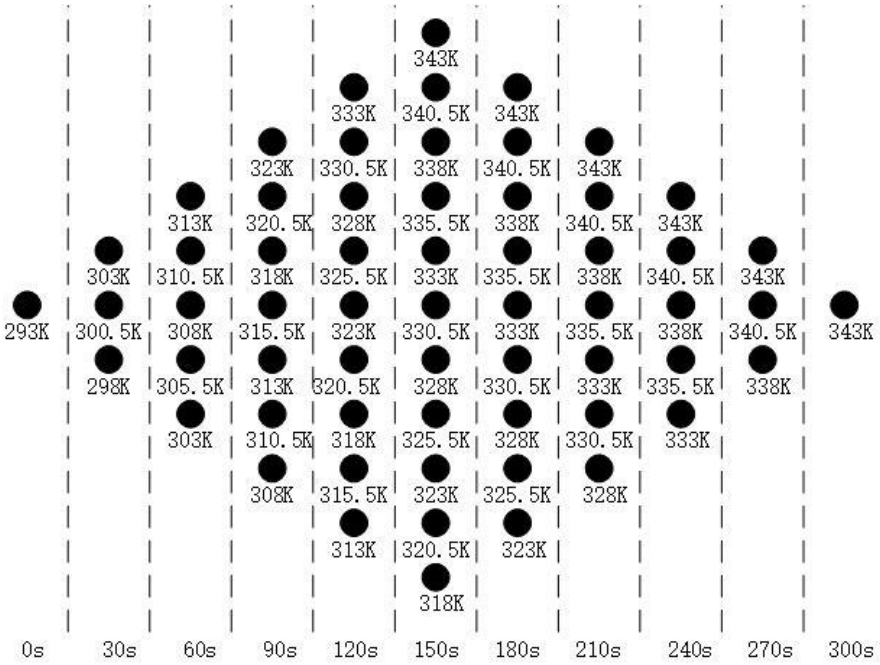

Figure 5. The definition of stage division and state variable of the dynamic programming model of the warm-up process.

Decision variable x_k is the expected coolant temperature-rise of each stage. If $s_k < 343$, then $x_k = \{5, 7.5, 10\}$; and if $s_k = 343$, then $x_k = 0$. Therefore, the dynamic programming state transition equation can be acquired as

$$s_{k+1} = s_k + x_k \tag{3}$$

The stage index function $v_k(s_k, x_k)$ is defined as the required fuel consumption for the expected coolant temperature increase x_k of each stage. Therefore, if the engine temperature $s_k < 343$ and the expected temperature increase is x_k during Stage x, then the required engine power output value $P_{ICE}(s_k, x_k/30)$ can be acquired according to the test results in Section 3. Moreover, in accordance with the test results in Chapter 1, the effective fuel consumption rate under the stage's initial temperature s_k and final temperature $s_k + x_k$ that correspond to the power output P_{ICE}, which are $b_e(P_{ICE}, s_k)$ and $b_e(P_{ICE}, s_k + x_k)$, respectively, can be obtained. To simplify the calculations, the linear average value

of $b_e(P_{ICE}, s_k)$ and $b_e(P_{ICE}, s_k + x_k)$ is used. If the engine temperature $s_k = 343$, then $v_k(s_k, x_k) = 0$. In summary, the stage index function can be expressed as

$$v_k(s_k, x_k) = \begin{cases} \frac{30P_{ICE}}{3600} \cdot \frac{b_e(P_{ICE}, s_k) + b_e(P_{ICE}, s_k + x_k)}{2}, s_k < 343 \\ 0, s_k = 343 \end{cases} \quad (4)$$

The process index function is the sum of the stage index functions:

$$f_k^*(s_k) = Min \sum_{i=k}^{11} v_i(s_i, x_i) \quad (5)$$

Therefore, the basic dynamic programming function can be acquired as

$$\begin{cases} f_{11}^*(s_{11}) = 0 \\ f_k^*(s_k) = \underset{x_k \in X_k(s_k)}{Min} \left\{ v_k(s_k, x_k) + f_{k+1}^*(s_{k+1}) \right\} \\ k = 10, 9, \ldots\ldots, 2, 1 \end{cases} \quad (6)$$

The control sequence for the minimal energy consumption of the warm-up process can be acquired by solving the dynamic programming model, as shown in Figure 6, where the expected rates of temperature increase are set as 0.167, 0.333 and 0.25 K/s at 0–60, 60–90 and 90–210 s, respectively. Then, the engine temperature is expected to reach 343 K after 210 s and to be maintained at this value until the ending point of the route, which is at 300 s.

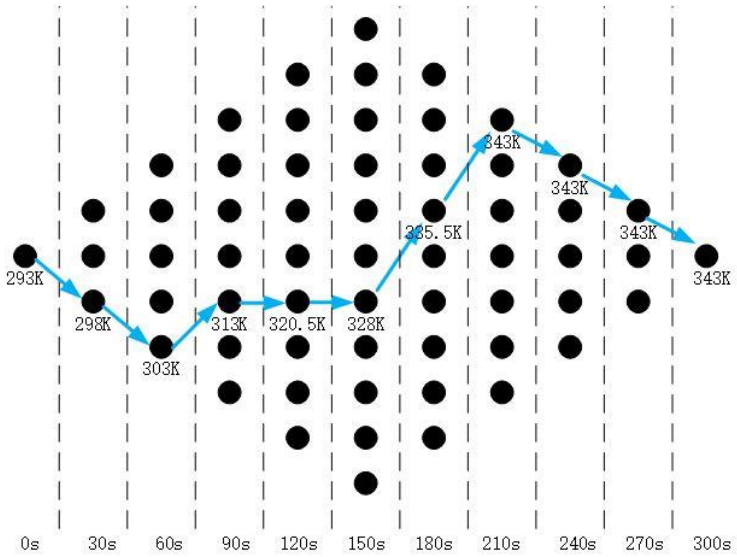

Figure 6. The optimal control sequence of the engine warm-up process acquired through dynamic programming.

5. Fuzzy Control Strategy

Through the adoption of dynamic programming, the power control sequence during the warm-up process with minimal energy consumption can be acquired without considering vehicle power output, the state of charge (SOC) of the battery and heat exchange between the internal combustion engine and the external environment. However, if these factors along with the difference in the rate of temperature increase due to air conditioning and the heater core are considered, then the degrees of freedom and the complexity of the system will be drastically increased, which is not advisable for off-line global optimization. Therefore, a fuzzy control strategy in serial HEV was designed in this research according

to engine temperature, the rate of change in engine temperature and the SOC of the battery, as shown in Figures 7 and 8.

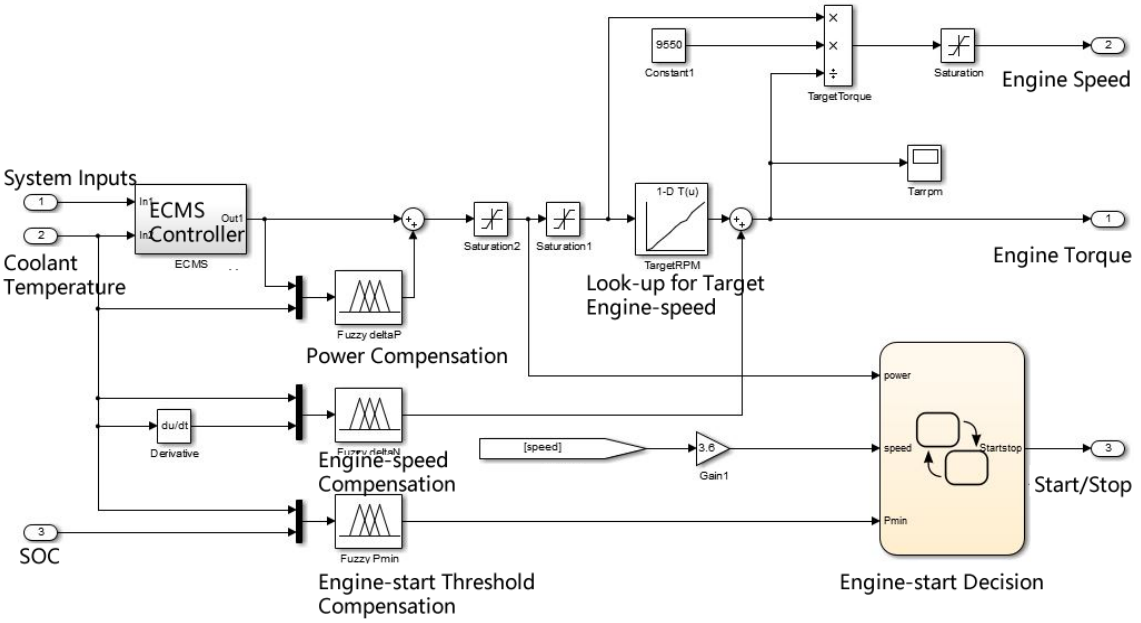

Figure 7. Fuzzy control model according to engine temperature.

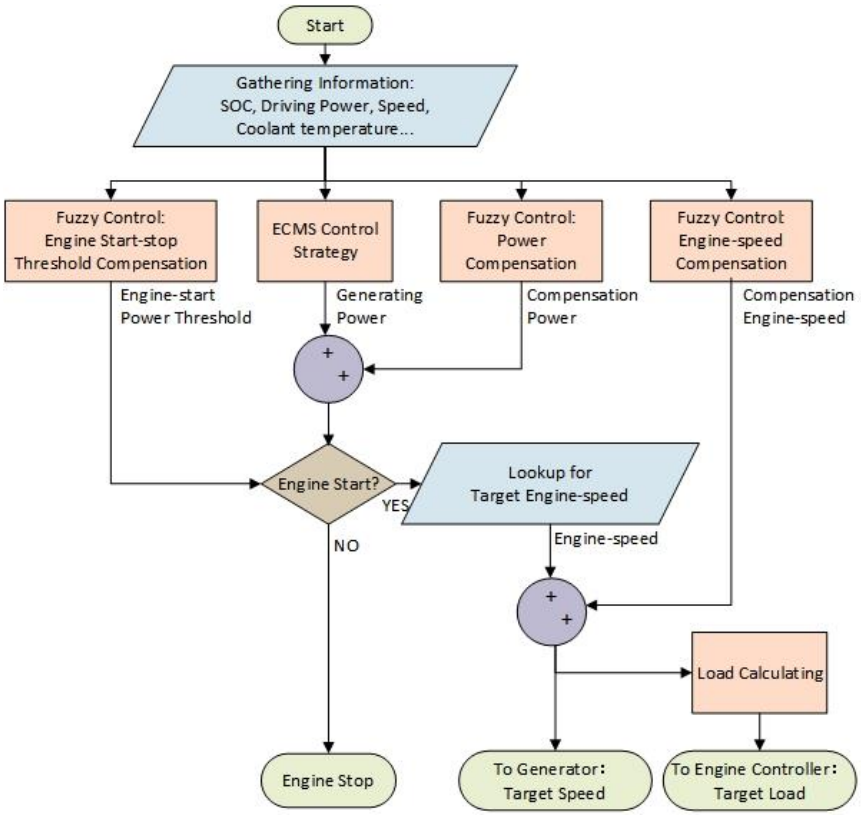

Figure 8. Flow diagram of the fuzzy control method according to engine temperature.

This control strategy is based on the ECMS instantaneous optimization method, and the influence of engine temperature is considered. During ECMS, engine temperature T_{ECT} is set as one of the

input variables, and the most efficient working condition range that corresponds to the current T_{ECT} is considered the optimal range. The corresponding specific fuel consumption b_e is acquired according to the current T_{ECT} during the calculation of the equivalent fuel consumption rate.

In the original ECMS control strategy, the output variable of the optimization algorithm is generally the expected engine power. Then, the control system compares the expected power with the start/stop threshold to determine whether the engine needs to be started. If the expected power is higher than start threshold, it will be used as the input to look up the table, which could determine the engine's target speed and target torque. In the ECMS + fuzzy control strategy that considers temperature, three fuzzy controllers were added, including a power compensation fuzzy controller, a speed compensation fuzzy controller, and a start-stop threshold fuzzy controller. The power compensation fuzzy controller acts on the stage of calculating the expected power, and its output variable will be added to the output of the original ECMS to become the final engine expected power. The start–stop threshold fuzzy controller acts on the engine start decision stage, and its output variable will change the power threshold for engine start. The engine speed fuzzy control will act on the stage of the target speed and torque calculation, and the engine speed or load will be adjusted without changing the engine power. Functions such as stabilizing cold-state engine speed, avoiding frequent cold start and stop, increasing engine warm-up speed, reducing fuel consumption and preventing engine from overheating under high-temperature conditions can be realized through the adoption of the three controllers.

(1) Power compensation fuzzy controller

The power compensation fuzzy controller is a dual-input single-output fuzzy control element, with the expected engine power P_{ICE} and temperature T_{ECT} from ECMS as inputs and the temperature compensating power P_{Corr} as the output. The actual target engine power P_{ICE_act} is the sum of the temperature compensating power and the expected engine power values:

$$P_{ICE\_act} = P_{ICE} + P_{Corr} \tag{7}$$

The input domain $P_{ICE} \in [0, 50]$ is divided into three membership functions: low, medium and high. Meanwhile, the input domain $T_{ECT} \in [-40, 120]$ is divided into five membership functions: ultra-low, low, medium, high and ultra-high. The output domain $P_{Corr} \in [-10, 10]$ is divided into five membership functions: negative big, negative, zero, positive and positive big.

The basic design theory of the fuzzy rule base is as follows. Under low-temperature conditions, if the expected engine power output is low, then positive power compensation is selected to increase engine warm-up speed. Under medium-temperature conditions, power compensation tends to become zero to fully realize the efficiency advantage of the ECMS instantaneous optimization method. Under high-temperature conditions, an adequate amount of negative power compensation is selected to prevent the engine from overheating. The final fuzzy rule after repeated calibrations is shown in Table 3. The Mamdani fuzzy inference system and the centre-of-gravity defuzzification method are adopted in the fuzzy controller, and the correlations between the output and inputs are shown in Figure 9.

Table 3. Fuzzy rule table for temperature compensating engine power.

P_{Corr}		P_{ICE}		
		L	**M**	**H**
T_{ECT}	UL	PB	Z	NB
	L	PB	Z	N
	M	P	Z	Z
	H	Z	Z	Z
	UH	Z	N	NB

UL—Ultra Low; L—Low; M—Middle; H—High; UH—Ultra High; PB—Positive Big; P—Positive; Z—Zero; N—Negative; NB—Negative Big.

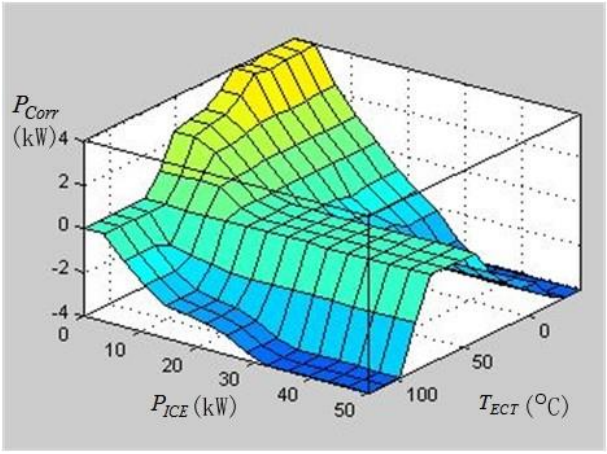

Figure 9. Output map of the power compensation fuzzy controller.

(2) Start/stop threshold fuzzy controller

The start/stop threshold fuzzy controller is a dual-input single-output fuzzy control element, with the battery SOC and engine temperature T_{ECT}(°C) as the inputs and the minimum power threshold $P_{\min}$ as the output. When $P_{ICE\_act} \geq P_{\min}$, the engine starts; when $P_{ICE\_act} < P_{\min} - 5$, the engine stops.

The input domain $SOC \in [0.3, 0.4]$ is divided into three membership functions: low, medium and high. Meanwhile, the input domain $T_{ECT} \in [-40, 120]$ is divided into five membership functions: ultra-low, low, medium, high and ultra-high. The output domain $P_{\min} \in [0, 15]$ is divided into four membership functions: high, medium, low and ultra-low.

The basic design theory of the fuzzy rule base is as follows. Under low-temperature conditions, if the expected engine power output is low, then low threshold values are selected to charge the battery, increase engine warm-up speed and avoid frequent starts and stops. During the engine warm-up process, the threshold value is increased to improve engine efficiency, whereas low threshold values are selected when battery SOC is low and vice versa. The fuzzy rule is summarised in Table 4, and the correlations between the output and inputs are illustrated in Figure 10.

Table 4. Fuzzy rule table for compensating start/stop threshold.

$P_{\min}$		SOC		
		L	**M**	**H**
T_{ECT}	UL	UL	UL	UL
	L	UL	UL	L
	M	L	L	M
	H	M	M	H
	UH	H	H	H

UL—Ultra Low; L—Low; M—Middle; H—High; UH—Ultra High; PB—Positive Big; P—Positive; Z—Zero; N—Negative; NB—Negative Big.

(3) Engine speed compensation fuzzy controller

Engine speed compensation is a dual-input single-output fuzzy control element, with the engine temperature T_{ECT}(°C) and the rate of change in engine temperature $\dot{T}_{ECT}$ as the inputs and engine speed compensation n_{Corr} as the output. The actual target engine speed n_{ICE_act} is the sum of the engine speed n_{ICE}, which corresponds to the target engine power output P_{ICE_act} and the engine speed compensation n_{Corr} values.

The input domain $T_{ECT} \in [-40, 120]$ is divided into five membership functions: ultra-low, low, medium, high and ultra-high. Meanwhile, the input domain $\dot{T}_{ECT} \in [-0.2, 0.6]$ is divided into four

membership functions: ultra-low, low, medium and high. The output domain $n_{Corr} \in [-200, 500]$ is divided into four membership functions: negative, zero, positive and positive big.

The basic design theory of the fuzzy rule base is as follows. When the temperature is below the ideal working temperature, high engine speed compensation values are selected to accelerate the warm-up process if the rate of change in engine temperature is low. If the rate of change in engine temperature increases, then the compensation level is decreased to keep the engine within efficient working conditions. When the temperature reaches the ideal value, negative compensation values are adopted to prevent the engine from overheating. The fuzzy rule is summarized in Table 5, and the correlations between the output and inputs are illustrated in Figure 11.

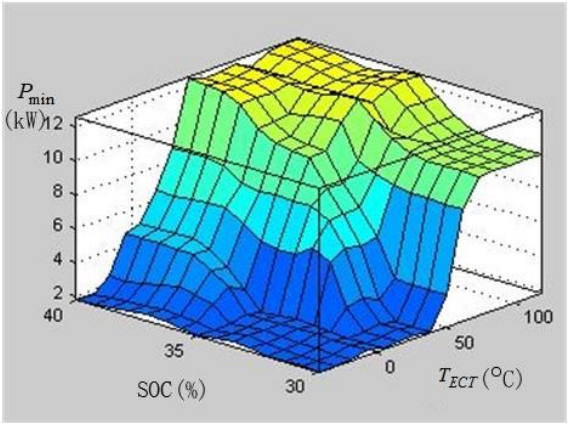

Figure 10. Output map of the start/stop threshold fuzzy controller.

Table 5. Fuzzy rule table for temperature compensating engine speed.

n_{Corr}		$\dot{T}_{ECT}$			
		UL	**L**	**M**	**H**
T_{ECT}	UL	PB	PB	P	P
	L	PB	P	Z	Z
	M	P	P	Z	Z
	H	Z	Z	N	N
	UH	Z	N	N	N

UL—Ultra Low; L—Low; M—Middle; H—High; UH—Ultra High; PB—Positive Big; P—Positive; Z—Zero; N—Negative; NB—Negative Big.

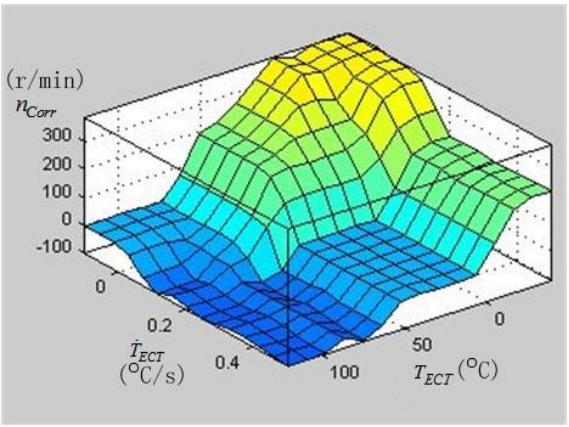

Figure 11. Output map of the engine speed compensation fuzzy controller.

6. Testing

During the test, the initial temperature of the engine coolant was set at an ambient temperature of 293 K and the initial SOC of the power battery was 30%. Two standardized cycle testing conditions, namely, the urban dynamometer driving schedule (UDDS) and the highway fuel economy test (HWFET), were selected for analysis.

The control strategies used include the ECMS control strategy that does not consider temperature, the ECMS control strategy with a fuzzy controller and the warming-up process control strategy based on dynamic programming. Among these, the warming-up process control strategy based on dynamic programming is divided into two phases according to coolant temperature: (1) when coolant temperature is lower than 343 K, the output power of the engine is controlled according to the optimization result of the dynamic programming; and (2) when coolant temperature is higher than 343 K, the engine output power is determined according to the conventional EMSC control strategy.

Most of the HEV energy management systems use the battery SOC as one of the inputs and affect the real-time power distribution. In order to perform comparative tests under similar initial conditions, we used the AVL e-Storage battery simulation system instead of a real battery. We set the capacity of the power battery, the open-circuit voltage curve at different SOCs and the internal resistance characteristic curve based on this system. During the experiment, the battery simulation system will change the output voltage according to the difference between the SOC and the load. At the same time, the voltage and current are integrated, and the assumed SOC is calculated with reference to the assumed battery capacity. In this way, we can create a relatively stable initial test condition.

The test results are summarized in Table 6. The engine output power, engine coolant temperature and fuel consumption under different control strategies are presented in Figures 12–14, respectively. Figures 15 and 16 show the outputs of the fuzzy controller when controlled by 'ECMS+ fuzzy control' under two test conditions.

First, we compare the original ECMS and ECMS with the fuzzy controller. In the UDDS cycle, which represents urban roads, the fuel consumption and battery consumption of the two strategies are almost the same, but with the fuzzy controller, the time for warm-up to 343 K is reduced by 28.1%, and the time for 363 K is reduced by 25.7%. In the case of the HWFET cycle, which represents highways, the energy consumption of the two strategies is also similar: ECMS with fuzzy controller can reduce fuel consumption by 1.6% and reduce battery consumption from −1.35 Ah to −1.38 Ah, i.e., the generated power is increased. At the same time, compared with the original ECMS control strategy, fuzzy controllers reduced the time warm-up to 343 K from 239 s to 131 s, which was shortened by nearly 45%.

Then, we compare the original ECMS and dynamic programming strategy. In the UDDS cycle, the battery consumption of the two control strategies is the same; however, the dynamic programming strategy reduces the fuel consumption from 583 g to 538 g, which is approximately 7.7%; at the same time, the dynamic programming strategy will also reduce the warm-up time to 343 K by 11.4%. In the HWFET cycle, the dynamic programming strategy reduced fuel consumption by approximately 10.0%, increased generated power by 3.7% and also shortened the warm-up time to 343 K by 15.5%.

For the above three control strategies, the end-of-test battery consumption was negative and the difference did not exceed 4%, indicating the existence of a battery usage surplus for the entire test. The energy management control strategy can effectively maintain the stability of the battery SOC and comply with the basic principles of energy management of hybrid electric vehicles.

Table 6. Warm-up time and energy consumption with different control strategies. ECMS: equivalent consumption minimization strategy; UDDS: urban dynamometer driving schedule; HWFET: highway fuel economy test.

Duty Cycle	Items	ECMS	ECMS + Fuzzy	Dynamic Programming (DP)
UDDS	Warm-up to 343 K/s	228	164	202
	Warm-up to 363 K/s	401	297	396
	Fuel Consumption/g	583	582	538
	Battery Consumption/Ah	−1.23	−1.22	−1.23
HWFET	Warm-up to 343 K/s	239	131	202
	Warm-up to 363 K/s	274	272	308
	Fuel Consumption/g	679	668	618
	Battery Consumption/Ah	−1.35	−1.38	−1.40

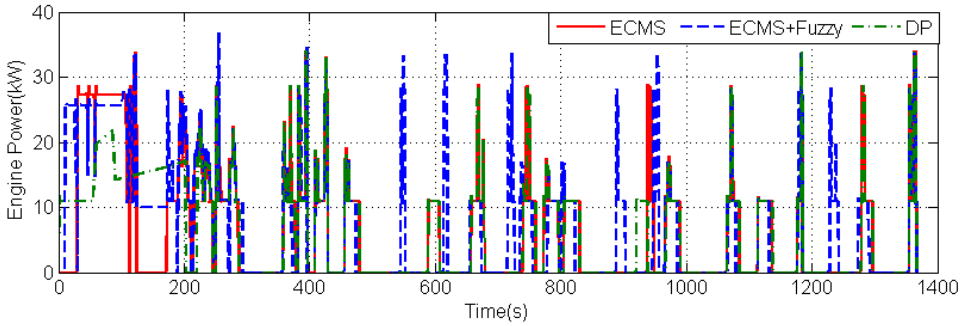

(**a**) UDDS

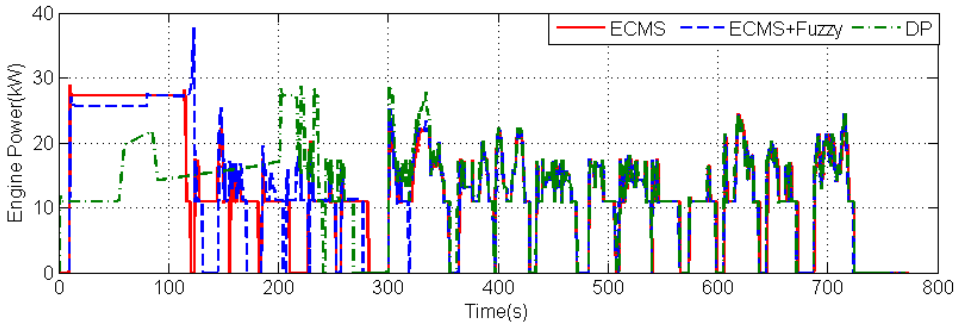

(**b**) HWFET

Figure 12. Auxiliary power unit (APU) output power with different control strategies.

With different control strategies, the plots of the engine output power are shown in Figure 12. In the first 300 s of the test—the engine warm-up process—the power output of different control strategies makes a significant difference; after warm-up, the power output tends to be consistent. During the warm-up process, the original ECMS control strategy tends to start and stop frequently. In the UDDS and HWFET cycle, the number of start-stops reached 8 and 6 before the coolant temperature reached 363 K. The ECMS + fuzzy control strategy reduces the engine power when the engine temperature is low (first 80 s) and maintains a certain power output during short-term parking, which causes the number of start-stops to reduce to 5. The dynamic programming strategy, in accordance with the optimization control sequence, avoids frequent start-stop during the whole warm-up process, and gradually increases the output power of the engine, which in turn, reduces the number of start-stops to 3 in UDDS and 2 in HWFET.

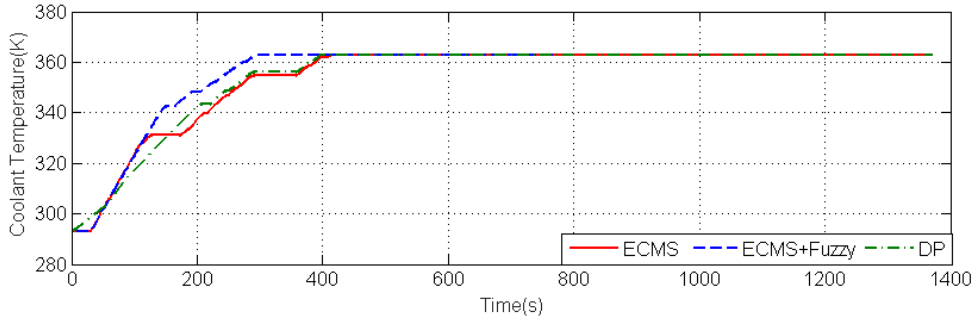

(**a**) UDDS

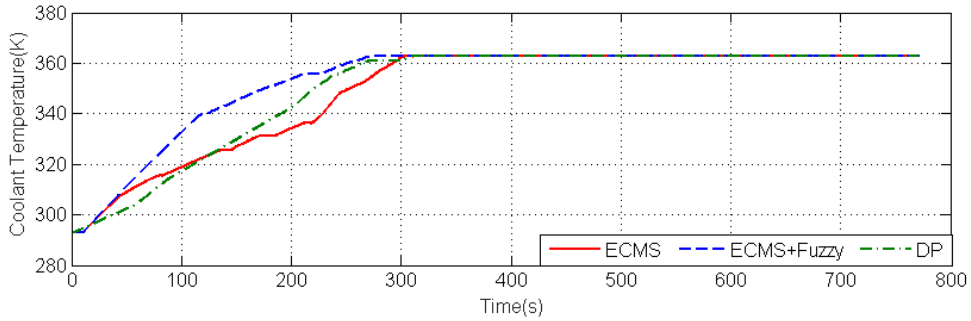

(**b**) HWFET

Figure 13. Coolant temperature with different control strategies.

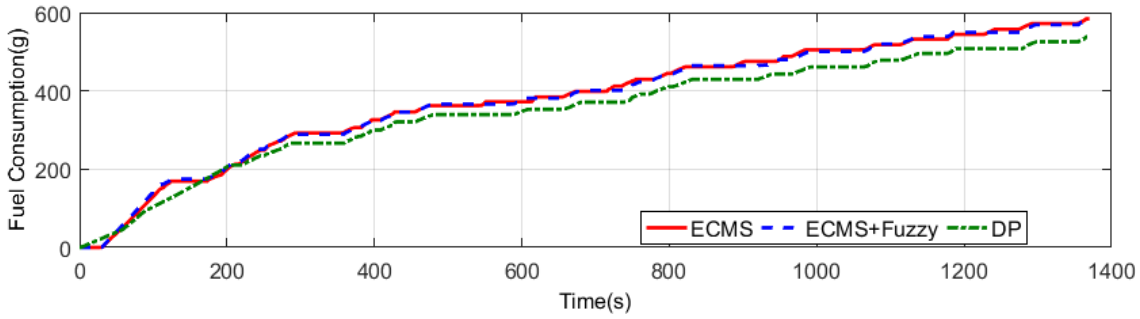

(**a**) UDDS

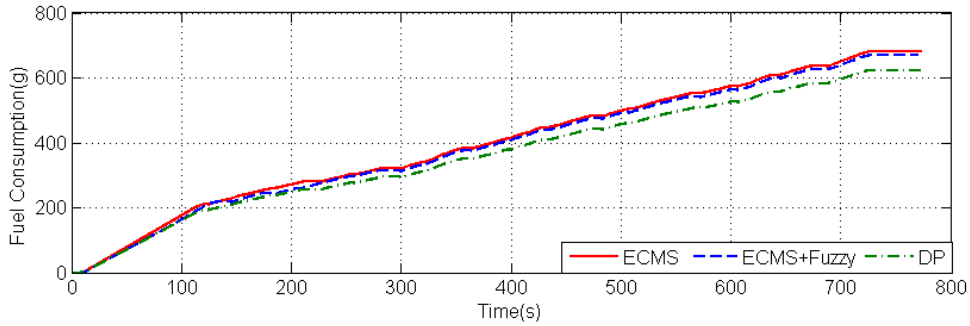

(**b**) HWFET

Figure 14. Fuel consumption with different control strategies.

For the different control strategies, the plots of coolant temperature and fuel consumption are shown in Figures 13 and 14, respectively. For the original ECMS, the coolant temperature and the fuel consumption both show a segmented increase because the power control tends to start and stop frequently and use a higher power output. The ECMS with fuzzy controller can increase the engine speed and maintain a longer engine run time when the coolant temperature is low, which corresponds

to the fastest temperature rise rate; but the fuzzy controllers do not affect to the output power of the engine to a large extent, so the fuel consumption of the ECMS and ECMS with or without the fuzzy controller is very similar. The dynamic programming strategy has a moderate and relatively stable temperature increase rate. This means that as the strategy outputs power in accordance with a predetermined control sequence, the warm-up time is basically the same, and the energy consumption is significantly less than the other two control strategies.

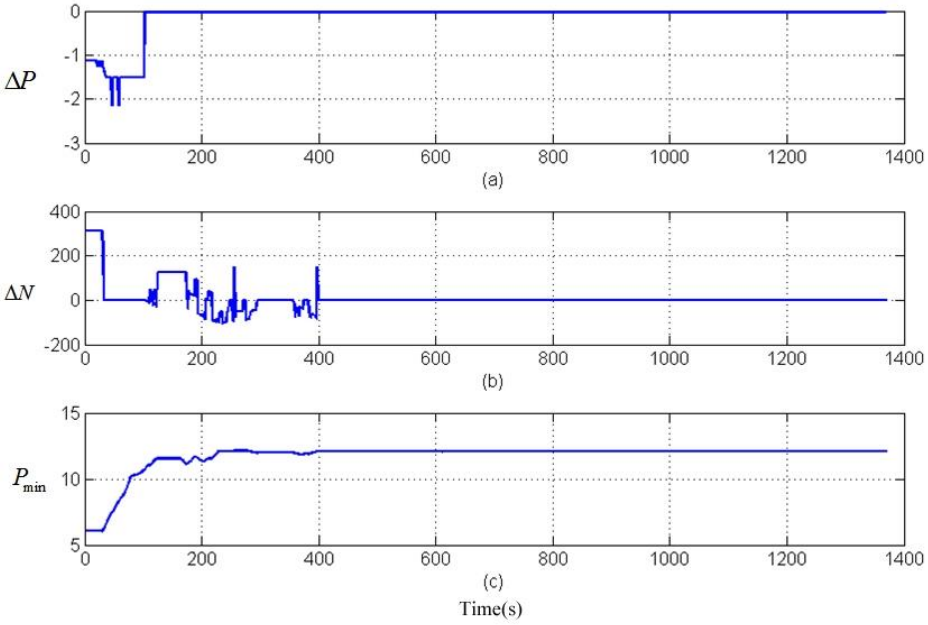

Figure 15. The fuzzy controller outputs under UDDS cycle.

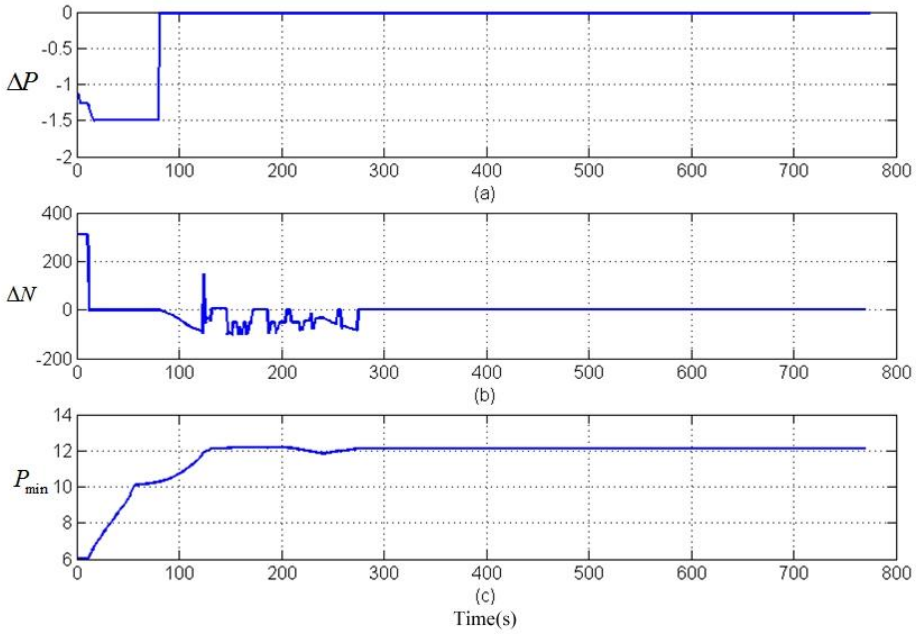

Figure 16. The fuzzy controller outputs under HWFET cycle.

In order to further understand the role of the fuzzy controller in the ECMS + Fuzzy Control strategy, the outputs of the three fuzzy controllers in the UDDS and HWFET cycles are shown in Figures 15 and 16. Observing the plots, it can be seen that the output of the fuzzy controllers during

the warm-up process is relatively stable regardless of the urban or highway conditions. When the coolant temperature is low (for the first 100 s), the fuzzy controllers will reduce the engine power by 1–2 kW, increase the engine speed up to 300 r/min and reduce the engine start threshold to 5 kW, thereby shortening the engine warm-up time. When the coolant temperature gradually approaches the ideal operating temperature (for the 100–200 s), the fuzzy controllers will no longer adjust the output power or start/stop threshold. In turn, it tends to properly reduce the engine speed, thereby increasing the efficiency of the engine. When the coolant temperature reaches the ideal range, the fuzzy controllers will no longer interfere with the ECMS control strategy. The above-mentioned output characteristics of the fuzzy controllers are highly consistent with the plots of the engine power, coolant temperature and fuel consumption as discussed earlier.

7. Conclusions

A significant increase in the fuel consumption of the engine was observed during the cold start and warm-up processes. Tests show that there are large differences in engine efficiency characteristics at different coolant temperatures, as well as the fact that coolant temperature rise rate increases with engine speed and engine load.

The time required for the engine warmer can be effectively shortened through a fuzzy control method aimed at the temperature of the coolant. Especially in an urban road environment represented by UDDS, an increase in the fuzzy control link can reduce the time required for the engine to heat to 343 K and 363 K by over 25% and simultaneously decrease the total fuel consumption in the test cycle.

The energy consumption during the warm-up process is significantly reduced through dynamic programming methods. Under UDDS working conditions, the duration of the warm-up process to 343 K can be shortened by approximately 10% through dynamic programming compared with the ECMS control strategy, which does not consider temperature. By contrast, under HWFET working conditions, the strategy based on dynamic programming increases the time required for the warm-up process. However, this strategy exhibits a significant advantage in terms of fuel economy in the case of the two driving cycles, where fuel consumption can be reduced by 10%.

Both warm-up process optimal control strategies, including fuzzy controller and dynamic programming, can meet the basic requirements of energy management strategies, such as maintaining battery SOC, and have different positive effects. In contrast, a dynamic programming strategy, which has the characteristics of reduced warm-up time and fuel consumption, is more suitable for normal climatic conditions; the ECMS with fuzzy controllers, despite the reduction in energy consumption not being obvious, can significantly shorten the warm-up time of the engine and is more suitable for cold environments or frequent short-distance driving conditions.

Author Contributions: Da Wang: designing the control strategies and writing manuscript; Chuanxue Song: organizing the research work and designing the control strategies; Yulong Shao: developing the control system; Shixin Song: testing and writing manuscript; Silun Peng: developing the control system and data analysis; Feng Xiao: designing and building the test bench.

Acknowledgments: This research is funded by the Key Tackling Item in Science and Technology Department of Jilin Province, China (No. 20150204017GX), Jilin Provincial Natural Science Foundation, China (No. 20150101037JC) and supported by Graduate Innovation Fund of Jilin University (No. 2017012).

Conflicts of Interest: The authors declare no conflict of interest.

References

1. Kanefsky, P.; Nelson, V.; Ranger, M. *A Systems Engineering Approach to Engine Cooling Design*; SAE International: Warrendale, PA, USA, 1999.
2. Hawley, J.G.; Bannister, C.D.; Brace, C.J.; Akehurst, S.; Pegg, I.; Avery, M.R. The effect of engine and transmission oil viscometrics on vehicle fuel consumption. *Proc. Inst. Mech. Eng. Part D J. Automob. Eng.* **2010**, *224*, 1213–1228. [CrossRef]

3. Luan, Y.; Henein, N.A.; Tagomori, M.K. *Port-Fuel-Injection Gasoline Engine Cold Start Fuel Calibration*; SAE International: Warrendale, PA, USA, 2006.
4. Roberts, A.; Brooks, R.; Shipway, P. Internal combustion engine cold-start efficiency: A review of the problem, causes and potential solutions. *Energy Convers. Manag.* **2014**, *82*, 327–350. [CrossRef]
5. Usman, A.; Park, C.W. Transient Lubrication of Piston Compression Ring during Cold Start-Up of SI Engine. *Int. J. Precis. Eng. Manuf.-Green Technol.* **2016**, *3*, 81–90. [CrossRef]
6. Alvarez, R.; Weilenmann, M. Effect of low ambient temperature on fuel consumption and pollutant and CO_2 emissions of hybrid electric vehicles in real-world conditions. *Fuel* **2012**, *97*, 119–124. [CrossRef]
7. Panday, A.; Bansal, H.O. Hybrid Electric vehicle Performance Analysis under Various Temperature Conditions. In *Clean, Efficient And Affordable Energy for a Sustainable Future*; Yan, J., Shamim, T., Chou, S.K., Li, H., Eds.; Elsevier: New York, NY, USA, 2015; Volume 75, pp. 1962–1967.
8. Cubito, C.; Millo, F.; Boccardo, G.; Di Pierro, G.; Ciuffo, B.; Fontaras, G.; Serra, S.; Garcia, M.O.; Trentadue, G. Impact of Different Driving Cycles and Operating Conditions on CO_2 Emissions and Energy Management Strategies of a Euro-6 Hybrid Electric Vehicle. *Energies* **2017**, *10*, 1590. [CrossRef]
9. Christenson, M.; Loiselle, A.; Karman, D.; Graham, L.A. *The Effect of Driving Conditions and Ambient Temperature on Light Duty Gasoline-Electric Hybrid Vehicles (2): Fuel Consumption and Gaseous Pollutant Emission Rates*; SAE International: Warrendale, PA, USA, 2007.
10. Lohse-Busch, H.; Duoba, M.; Rask, E.; Stutenberg, K.; Gowri, V.; Slezak, L.; Anderson, D. *Ambient Temperature (20°F, 72°F and 95°F) Impact on Fuel and Energy Consumption for Several Conventional Vehicles, Hybrid and Plug-In Hybrid Electric Vehicles and Battery Electric Vehicle*; SAE International: Warrendale, PA, USA, 2013.
11. Haupt, C.; Buecherl, D.; Engstle, A.; Herzog, H.G.; Wachtmeister, G. Energy management in hybrid vehicles considering thermal interactions. In Proceedings of the 2007 IEEE Vehicle Power and Propulsion Conference (VPPC 2007), Arlington, TX, USA, 9–12 September 2007; pp. 36–41.
12. Zhao, J.; Wang, J. Integrated Model Predictive Control of Hybrid Electric Vehicles Coupled With Aftertreatment Systems. *IEEE Trans. Veh. Technol.* **2016**, *65*, 1199–1211. [CrossRef]
13. Tian, Y.; Sun, W.; Qu, D.; Wang, L. Study of a Exhaust After-treatment System Applied to Hybrid Vehicle. In Proceedings of the 2011 Asia-Pacific Power And Energy Engineering Conference, Wuhan, China, 25–28 March 2011.
14. Jeffers, M.A.; Chaney, L.; Rugh, J.P. Climate Control Load Reduction Strategies for Electric Drive Vehicles in Cold Weather. *SAE Int. J. Passeng. Cars—Mech. Syst.* **2016**, *9*, 75–82.
15. Tashiro, T. Power Management of a Hybrid Electric Vehicle During Warm-up Period Considering Energy Consumption of Cabin Heat Components. *IFAC PapersOnLine* **2016**, *49*, 393–398. [CrossRef]
16. Hu, T.; Inderwisch, K.; Mustafa, R.; Küçükay, F. *Research on the Optimization of Hybrid Electric Vehicle Powertrain Heating-Up Process*; SAE International: Warrendale, PA, USA, 2013.
17. Shidore, N.; Rask, E.; Vijayagopal, R.; Jehlik, F.; Kwon, J.; Ehsani, M. PHEV Energy Management Strategies at Cold Temperatures with Battery Temperature Rise and Engine Efficiency Improvement Considerations. *SAE Int. J. Engines* **2011**, *4*, 1007–1019. [CrossRef]
18. Dubouil, R.; Hetet, J.F.; Maiboom, A. *Modelling of the Warm-Up of a Spark Ignition Engine: Application to Hybrid Vehicles*; SAE International: Warrendale, PA, USA, 2011.
19. Jehlik, F.; Rask, E.; Christenson, M. *Simplified Methodology for Modeling Cold Temperature Effects on Engine Efficiency for Hybrid and Plug-in Hybrid Vehicles*; SAE International: Warrendale, PA, USA, 2010.
20. Solouk, A.; Shahbakhti, M. Energy Optimization and Fuel Economy Investigation of a Series Hybrid Electric Vehicle Integrated with Diesel/RCCI Engines. *Energies* **2016**, *9*, 1020. [CrossRef]
21. Alaoui, C.; Salameh, Z.M. A novel thermal management for electric and hybrid vehicles. *IEEE Trans. Veh. Technol.* **2005**, *54*, 468–476. [CrossRef]
22. Graham, L.; Christenson, M.; Karman, D. Light duty hybrid vehicles—Influence of driving cycle and operating temperature on fuel economy and GHG emissions. In Proceedings of the 2006 IEEE EIC Climate Change Technology, Ottawa, ON, Canada, 10–12 May 2006.
23. Smith, R.; Morison, M.; Capelle, D.; Christie, C.; Blair, D. GPS-based optimization of plug-in hybrid electric vehicles' power demands in a cold weather city. *Transp. Res. Part D Transp. Environ.* **2011**, *16*, 614–618. [CrossRef]
24. Kim, N.; Cha, S.; Peng, H. Optimal Control of Hybrid Electric Vehicles Based on Pontryagin's Minimum Principle. *IEEE Trans. Control Syst. Technol.* **2011**, *19*, 1279–1287.

25. Kim, N.; Cha, S.W.; Peng, H. Optimal Equivalent Fuel Consumption for Hybrid Electric Vehicles. *IEEE Trans. Control Syst. Technol.* **2012**, *20*, 817–825.
26. Sciarretta, A.; Guzzella, L. Control of hybrid electric vehicles. *IEEE Control Syst. Mag.* **2007**, *27*, 60–70. [CrossRef]
27. Serrao, L.; Onori, S.; Rizzoni, G. ECMS as a realization of Pontryagin's minimum principle for HEV control. In Proceedings of the 2009 IEEE American Control Conference, St. Louis, MO, USA, 10–12 June 2009; pp. 3964–3969.
28. Gao, W.; Zou, Y.; Sun, F. Optimal Component Sizing for a Parallel Hybrid Bus Based on Dynamic Programming. In Proceedings of the 2014 IEEE Conference and Expo Transportation Electrification Asia-Pacific (ITEC Asia-Pacific), Beijing, China, 31 August–3 September 2014.
29. Yuan, Z.; Teng, L.; Sun, F.; Peng, H. Comparative Study of Dynamic Programming and Pontryagin's Minimum Principle on Energy Management for a Parallel Hybrid Electric Vehicle. *Energies* **2013**, *6*, 2305–2318. [CrossRef]